

Unusual, Vesicle-like Patterned, Mesoscopically Ordered Silica

Anna Lind,[†] Bernd Spliethoff,[‡] and Mika Lindén^{*,†}

Department of Physical Chemistry, Åbo Akademi University, Porthansgatan 3-5,
FIN-20500 Turku, Finland, and Max-Planck-Institut für Kohlenforschung,
Kaiser-Wilhelm-Platz 1, D-45470, Mülheim an der Ruhr, Germany

Received June 25, 2002. Revised Manuscript Received November 19, 2002

A mixture of cationic and anionic surfactants has been used as structure-directing agents in the synthesis of mesoscopically ordered silica in the presence of toluene. The preferred interfacial curvature was adjusted by varying the anionic/cationic surfactant molar ratio, which allowed for better control of the solubilization of toluene by the silicate–surfactant mesophase. A pronounced increase in the toluene solubilization capacity was observed at anionic/cationic surfactant molar ratios close to that where the lamellar phase starts to appear in the absence of added toluene. TEM measurements reveal the presence of long, vesicular structures in the materials synthesized in the presence of anionic/cationic surfactant and toluene. Apart from TEM measurements, the materials were characterized by SAXS, N₂ sorption, and ²⁹Si NMR.

Introduction

The solubilization of a hydrophobic agent inside the hydrophobic portion of ordered anionic silicate–cationic surfactant mesophases has been widely used to increase the pore size of the final material.^{1–4} Usually aromatic hydrocarbons, like trimethylbenzene, TMB, have been used for this purpose. In situ studies reveal that the surfactant–silicate mesophase is able to solubilize large amounts of swelling agent after it has formed, stressing the nonequilibrium nature of the solubilization process.⁵ However, the silicate condensation sets a limit for the solubilization capacity, and at higher degrees of silicate condensation the solubilization capacity is completely lost.^{2,3,5} The solubilization of a swelling agent inside the core of the supramolecular surfactant assembly leads to a decrease in the interfacial curvature of the aggregate.

To clarify the influence of the interfacial curvature of the surfactant aggregates on the solubilization behavior of the silicate–surfactant mesophase, we have recently studied the solubilization of toluene by a silicate mesophase where a mixture of cationic (CTAB) and anionic (decanoic acid) surfactants was used as the structure-directing agent.⁶ In the alkaline conditions of

the synthesis the decanoic acid will completely dissociate into the decanoate form. The motivation for the use of a mixture of oppositely charged surfactants was to decrease the preferred interfacial curvature of the mixed supramolecular aggregates in a controlled way,^{7–9} to enhance the solubilization capacity. Indeed, the lower preferred interfacial curvature of mixed decanoate/hexadecyltrimethylammonium bromide (CTAB) complexes compared to that of CTAB alone lead to an increased TEOS/toluene solubilization capacity. Again, a pronounced uptake of toluene by the mesophase occurred after the formation of the hexagonal phase. However, the *d*spacing of the initially formed hexagonal phase increased with increasing decanoic acid/CTAB ratio, suggesting that some toluene has already been solubilized by the silicate–surfactant micellar entities before the assembly of the mesophase. Furthermore, smaller silicate–surfactant particles are formed, compared to those observed in the absence of anionic cosurfactant, most probably due to the fact that more nucleation sites are being produced in the highly dispersed catanionic system.⁶ This article is concerned with the characterization of the thus-synthesized powderous porous solids.

Experimental Section

Materials. The following chemicals were used in the synthesis: hexadecyltrimethylammonium bromide (CTAB) and tetraethyl orthosilicate (TEOS) were obtained from Aldrich. Decanoic acid and toluene were supplied by Fluka and ammonia (25%) by J. T. Baker. All chemicals were used as received. The water was purified by distillation and deionization.

* To whom correspondence should be addressed.

[†] Åbo Akademi University.

[‡] Max-Planck-Institut für Kohlenforschung.

(1) Kresge, C. T.; Leonowicz, M. E.; Roth, W. J.; Vartuli, J. C. *Nature* **1992**, *359*, 170.

(2) Beck, J. S.; Vartuli, J. C.; Roth, W. J.; Leonowicz, M. E.; Kresge, C. T.; Schmitt, K. D.; Chu, C. T.-W.; Olson, D. H.; Sheppard, E. W.; McCullen, S. B.; Higgins, J. B.; Schlenker, J. L. *J. Am. Chem. Soc.* **1992**, *114*, 10834.

(3) Huo, Q.; Margolese, D. I.; Ciesla, U.; Demuth, D.; Feng, P.; Gier, T. E.; Sieger, P.; Firouzi, A.; Chmelka, B. F.; Schüth, F.; Stucky, G. D. *Chem. Mater.* **1994**, *6*, 1176.

(4) Ulagappan, N.; Rao, C. N. R. *Chem. Commun.* **1996**, 2759.

(5) Lindén, M.; Ågren, P.; Karlsson, S.; Bussian, P.; Amenitsch, H. *Langmuir* **2000**, *16*, 5831.

(6) Lind, A.; Andersson, J.; Karlsson, S.; Ågren, P.; Bussian, P.; Amenitsch, H.; Lindén, M. *Langmuir* **2002**, *18*, 1380.

(7) Chen, F.; Huang, L.; Li, Q. *Chem. Mater.* **1997**, *9*, 2685.

(8) Chen, F.; Yan, X.; Li, Q. *Stud. Surf. Sci. Catal.* **1998**, *117*, 273.

(9) Chen, F.; Song, F.; Li, Q. *Microporous Mesoporous Mater.* **1999**, *29*, 315.

Synthesis. CTAB ($m = 2.4$ g) and decanoic acid were dissolved in water ($m = 120$ g) by stirring (500 rpm) at 30 °C. After complete dissolution of the CTAB and the decanoic acid, 10 mL of 25% NH_3 was added and the solution stirred for about 5 min. The pH was adjusted by addition of NaOH ($[\text{Na}^+] \ll [\text{NH}_4^+]$). Toluene was then added to the synthesis mixture, which was stirred for another 5 min. TEOS ($m = 9.4$ g) was rapidly added to the solution, which was stirred for 1 h. The final molar composition was 157/3/0.15/1/ x/y $\text{H}_2\text{O}/\text{NH}_3/\text{CTAB}/\text{TEOS}/\text{decanoic acid}/\text{toluene}$. In standard synthesis, with no decanoic acid added, the pH before addition of TEOS is 11.8. When decanoic acid was added to the synthesis, the pH was adjusted to 11.8 by addition of 1 M NaOH before addition of TEOS, if not otherwise mentioned. After addition of TEOS the pH decreased to 10.7 in all cases. The material was aged in the mother liquid at pH 8 in 90 °C for 6 days, to be stable for calcination. The pH was adjusted by addition of acetic acid. After aging, the material was isolated by filtration and dried overnight at 90 °C. Calcination was performed under air at 550 °C for 5 h with a heating ramp of 1 °C/min.

X-ray Analysis. Small-angle X-ray scattering (SAXS) measurements were performed on a Kratky compact small-angle system. A Seifert ID-3003 X-ray generator, operating at a maximum intensity of 50 kV and 40 mA, provided the Cu $K\alpha$ radiation of wavelength 1.542 Å. A Ni filter was used to remove the $K\beta$ radiation, and a W filter was used to protect the detector from the primary beam. The system was equipped with a position-sensitive detector measuring up to 9° 2θ with a sensitivity of 0.01°. The sample-to-detector distance was 277 mm. To minimize the background scattering from air, the camera volume was kept under vacuum during the measurements.

N_2 Sorption Analysis. The N_2 isotherms were determined at 77 K using a Micromeritics ASAP 2010 sorptometer. The aged and calcined samples were outgassed at 423 K before measurements.

^{29}Si MAS NMR. The ^{29}Si magic-angle spinning (MAS) NMR experiments were carried out using a 270-MHz Chemagnetics CMX Infinity spectrometer using a home-built 10-mm NMR probe. The spectra were acquired using a 30° excitation pulse, a 300-s recycle delay, about 400 transients, and a MAS speed of about 4 kHz. The chemical shifts were referenced to trimethylsilane (TMS) using a secondary reference of 3-(trimethylsilyl)propanesulfonic acid sodium salt (+1.6 ppm).

Transmission Electron Microscopy. A Hitachi HF 2000 transmission electron microscope operated at 200 keV was used, which was equipped with a cold field emission source. Samples were mounted on carbon films that were fixed on copper grids.

Results

SAXS Measurements. The transparent, isotropic micellar solution of low viscosity containing CTAB, water, and ammonia turned increasingly more viscous upon addition of decanoic acid, before the addition of TEOS. This is to be expected for micellar solutions that undergo a sphere-to-rod transition. A white precipitate formed within the first minutes after addition of TEOS to the micellar solution. For the pure CTAB solutions a well-ordered hexagonal phase was formed with a d_{100} spacing of the as-synthesized, wet sample of 4.3 nm. Increasing the decanoic acid/CTAB molar ratio, m , leads to a gradual increase in the d spacing of the hexagonal phase to 4.7 nm at $m = 0.53$. A hexagonal-to-lamellar phase transition was observed with increasing m through a compositional region where the two phases coexist, as shown in Figure 1. The lamellar phase starts to appear in the XRD diffractogram at $m = 0.35$. As for the hexagonal phase, the d spacing of the lamellar phase also increased slightly with increasing m . The solubi-

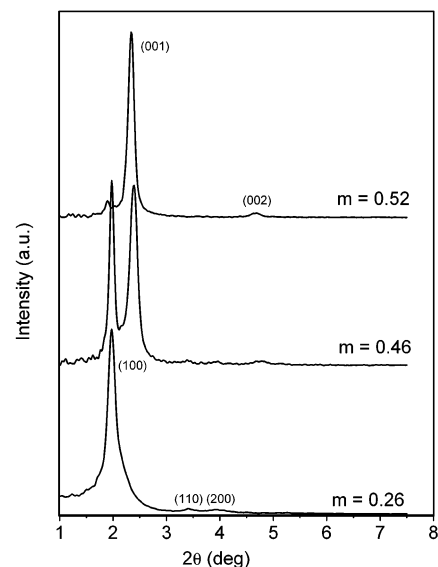


Figure 1. XRD patterns of decanoic acid/CTAB templated mesoscopic silica as a function of decanoic acid/CTAB molar ratio, m .

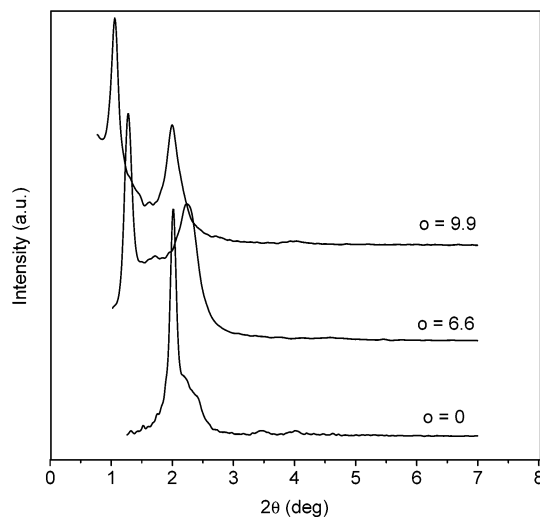


Figure 2. XRD patterns of decanoic acid/CTAB templated mesoscopic silica as a function of toluene/CTAB molar ratio, o , at a constant decanoic acid/CTAB molar ratio, m , of 0.35.

lization of toluene by the decanoate/CTAB–silica composite was studied as a function of toluene/CTAB molar ratio, o , and the decanoic acid/CTAB molar ratio, m , respectively. Solubilization of toluene led to a swelling of both the hexagonal and the lamellar phase, and the degree of swelling increased with increasing toluene concentration, as shown in Figure 2. At a constant CTAB/toluene molar ratio, an almost linear dependence of the d spacing of the hexagonal phase on m was observed up to $m = 0.35$. However, at $m > 0.35$ a transition to another linear region was observed for $o = 9.9$ with a higher degree of swelling compared to that observed at m values below 0.35, as shown in Figure 3, in line with our recently published in situ SAXS study on the same system.⁶ This breaking point is less obvious for samples with $o = 6.6$. It is interesting to note, however, that the m value of 0.35 is very closely corresponding to that needed for the lamellar phase to appear in the SAXS diffractograms of samples synthesized in the absence of toluene.

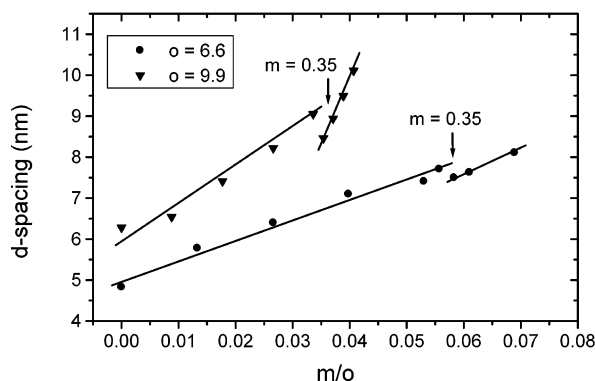


Figure 3. Observed d_{100} spacings of the hexagonal phase of decanoic acid/CTAB templated mesoscopic silica as a function of decanoic acid/toluene molar ratio, m/o , and toluene/CTAB molar ratio, o .

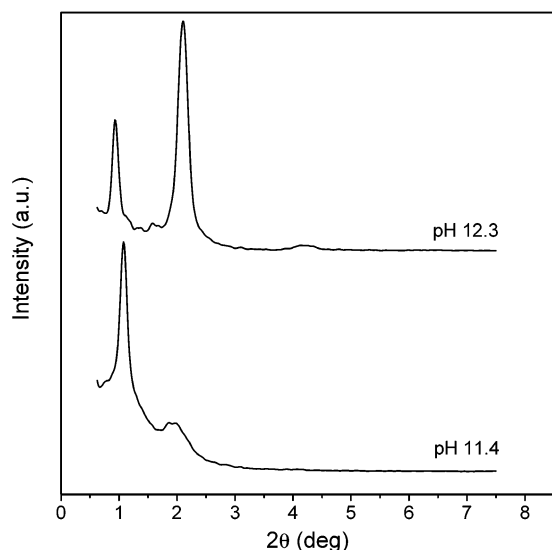


Figure 4. XRD patterns of decanoic acid/CTAB templated mesoscopic silica at a constant decanoic acid/CTAB molar ratio $m = 0.35$ and toluene/CTAB molar ratio $o = 9.9$ as a function of synthesis pH.

It has previously been shown that the solubilization of a hydrophobic agent by a developing silicate–surfactant mesophase is suppressed by an increase in the degree of silicate condensation.^{2,3,5,6} Therefore, solubilization experiments were also carried out at higher pHs since it is well-known that the silicate condensation rate is lowered with increasing pH under alkaline conditions.^{10,11} Increasing the pH led to an increase in the fraction of lamellar phase, as shown in Figure 4. However, increasing the pH above 11.8 also led to a pronounced swelling of the coexisting hexagonal phase, as shown in Figure 5. At a higher toluene concentration, the d spacing of the lamellar phase decreased when increasing the synthesis pH, whereas the fraction of swollen hexagonal phase increased. At a lower toluene concentration, however, increasing the pH gives a swelling of the lamellar phase. However, it is clear that the extent at which the swollen hexagonal phase and the lamellar phase, respectively, appear in the diffractogram is connected to both hydrodynamic effects as

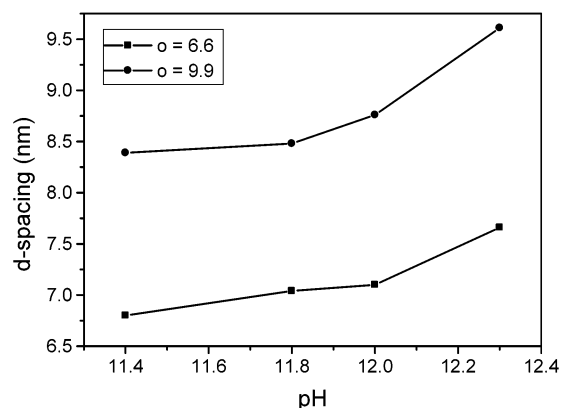


Figure 5. Observed d_{100} spacings of the hexagonal phase of decanoic acid/CTAB templated mesoscopic silica as a function of synthesis pH and toluene/CTAB molar ratio, o , at a constant decanoic acid/CTAB molar ratio $m = 0.35$.

Table 1. ^{29}Si NMR Data for Dried, Both As-Synthesized and Aged Material, Studied for Different Decanoic Acid/CTAB Molar Ratios, m , and Toluene/CTAB Molar Ratios, o

m	o		Q^2	Q^3	Q^4	Q^4/Q^3
0	0	as-synthesized	5.6	35.9	58.5	1.6
0.35	0	as-synthesized	5.4	34.8	59.8	1.7
0.35	9.9	as-synthesized	6.6	31.3	62.0	2.0
0.35	9.9	aged	2.7	16.9	80.3	4.8

well as to the rate of silicate condensation since, under the experimental conditions applied, the higher the stirring rate and the lower the pH, the larger is the fraction of swollen hexagonal phase in the diffractograms. Furthermore, it has previously been shown that a increased oil solubilization capacity of anionic poly-electrolyte and cationic surfactant complexes can be achieved by increasing the charge density of the poly-electrolyte.¹² Therefore, charge density effects can also have an influence on the observed swelling of the hexagonal silicate–surfactant phase when going toward higher pH values. Increasing the pH above 12 will lead to a higher charge density of the anionic polysilicate species.

The materials obtained from the synthesis described above lost their mesoscopic order upon calcination, which is attributable to the thin pore walls in combination with a large pore diameter. The as-synthesized materials were therefore aged at pH = 8 and 90 °C for 6 days to increase the degree of silicate condensation and thus the thermal stability of the mesophase. The corresponding Q^4/Q^3 ratios, as determined by ^{29}Si NMR, are summarized in Table 1. The Q^4/Q^3 ratios measured for the as-synthesized, dried materials ranged between 1.6 and 2.0, regardless of the synthesis composition. Similar values have been observed for as-synthesized mesostructured silica in other studies.¹³ However, the Q^4/Q^3 ratios for the aged samples were substantially higher, around 5. Despite the pronounced increase in the degree of condensation, no change in the d spacing of the hexagonal phase was observed, even after removal of the organic portion by calcination, as illustrated in Figure 6. However, the d_{001} reflection of the lamellar

(10) Brinker, C. J.; Scherer G. W. *Sol–Gel Science*; Academic Press: San Diego, 1990.

(11) Gross, A. F.; Le, V. H.; Kirsch, B. L.; Riley, A. E.; Tolbert, S. H. *Chem. Mater.* **2001**, *13*, 3571.

(12) Hayakawa, K.; Tanaka, R.; Kurawaki, J.; Kusumoto, Y.; Satake, I. *Langmuir* **1999**, *15*, 4213.

(13) Kim, S.-S.; Liu, Y.; Pinnavaia, T. J. *Microporous Mesoporous Mater.* **2001**, *44–45*, 489.

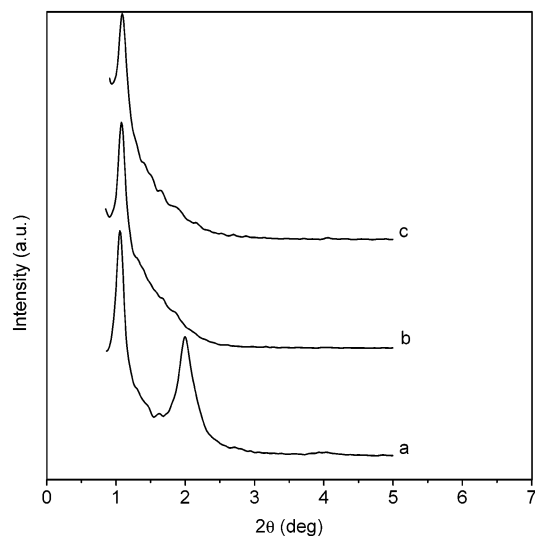


Figure 6. XRD patterns of decanoic acid/CTAB templated mesoscopic silica at a constant decanoic acid/CTAB molar ratio $m = 0.35$ and toluene/CTAB molar ratio $o = 9.9$. (a) As-synthesized, wet sample; (b) aged, wet sample; (c) aged, calcined sample.

phase present for materials synthesized at higher decanoic acid/CTAB molar ratios disappeared after aging of the materials.

Transmission Electron Microscopy. Aged and calcined samples were investigated by TEM. A representative image of a material synthesized at $m = 0$ and $o = 9.9$ is shown in Figure 7a. The material is very well ordered with a hexagonal packing close to hexagonally shaped pores. The repeat distance correlates very well with that observed in the XRD, as expected. The seemingly lamellar structures seen in Figure 7a originate from a side view of the silica tubes building up the hexagonal mesophase.

The material structure, as seen under the TEM, was changed quite remarkably as the decanoic acid/CTAB ratio was increased, especially at m values exceeding 0.35. In Figure 7b a picture of a material synthesized at $m = 0.40$ and $o = 9.9$ is shown as an example. Well-ordered regions possessing a hexagonal symmetry were still observed, with d spacings in nice agreement with those observed in the XRD. However, extended, thin, and highly curved, vesicle-like structures, several micrometers in length, were also observed, the occurrence of which generally increased with increasing value of m . However, fractions of a vesicle-like structure were also observed to a limited extent in the TEM images for the material synthesized at $o = 9.9$ and $m = 0$.

N₂ Sorption. The materials synthesized can be divided into three main groups, depending on their toluene solubilization capacity during the synthesis and the N₂ sorptive properties of the calcined materials, respectively. The BET surface area was $580 \pm 50 \text{ m}^2/\text{g}$, which is lower than that for standard MCM-41 material, as can be expected for materials with larger pores. An estimation of the pore volume is difficult to make since none of the isotherms terminate in a plateau at high relative pressures. Typical isotherms representative of the main groups A, B, and C are shown in Figure 8. (See figure captions for details on the synthesis composition.) The isotherm representative of each group will be discussed separately below.

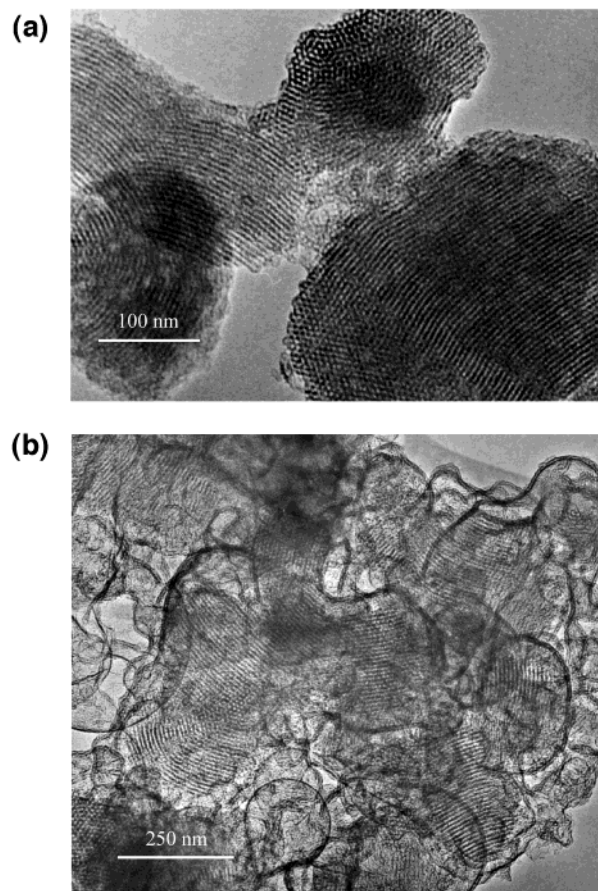


Figure 7. TEM image of material synthesized at (a) decanoic acid/CTAB molar ratio 0 and toluene/CTAB molar ratio 9.9 and (b) decanoic acid/CTAB molar ratio 0.40 and toluene/CTAB molar ratio 9.9.

A. An isotherm typical for this group was obtained for materials synthesized in the absence of decanoic acid at $o = 6.6$ and $o = 9.9$. This isotherm shows a marked uptake between $p/p_0 = 0.3$ and $p/p_0 = 0.45$, indicative of mesopores with a narrow pore size distribution around 3.5 nm, as calculated according to the commonly applied BJH method. The second marked uptake observed at high relative pressures can be attributed to textural porosity. The hysteresis seen above $p/p_0 = 0.5$ could indicate the presence of larger pores connected via smaller openings, and interparticle voids, which could be understandable if the solubilization of toluene would lead to pore wall corrugation.¹⁴ However, the hysteresis observed at relative pressures >0.5 could imply that there is a swelling of the material with increasing relative pressure due to nonrigid textural porosity.

B. An isotherm typical for materials synthesized at $o = 6.6$ and $m = 0.35$ for different synthesis pH, and at $o = 9.9$ and $m < 0.35$, shows a less steep uptake in the adsorption at about $p/p_0 = 0.4-0.7$ together with a hysteresis loop. The BJH-pore diameter estimated from the desorption branch was 2.5–5 nm, depending on the degree of swelling of the mesophase. Again, a marked textural porosity was observed, as evidenced by the pronounced uptake at high relative pressures.

(14) Desplandier-Giscard, D.; Galarneau, A.; Di Renzo, F.; Fajula, F. *Stud. Surf. Sci. Catal.* **2001**, *135*, 205.

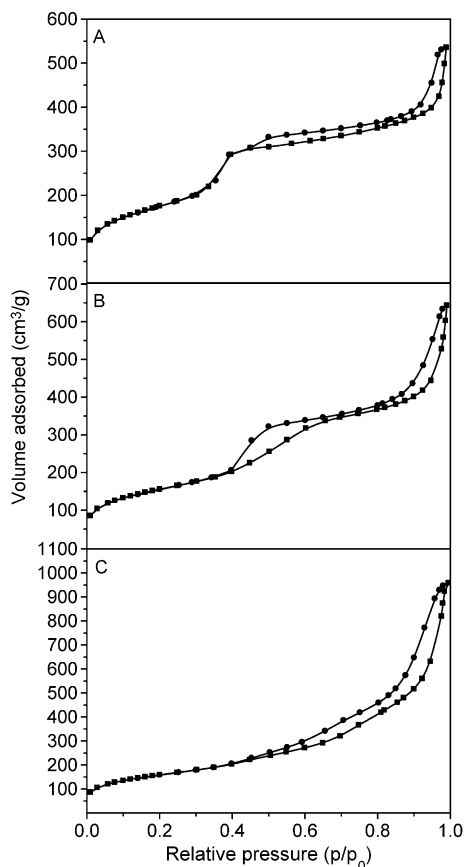


Figure 8. N_2 sorption isotherms representing the three groups: (A) decanoic acid/CTAB molar ratio 0 and toluene/CTAB molar ratio 6.6; (B) decanoic acid/CTAB molar ratio 0.35 and toluene/CTAB molar ratio 6.6; (C) decanoic acid/CTAB molar ratio 0.40 and toluene/CTAB molar ratio 9.9.

C. Samples with $o = 9.9$ and $m \geq 0.35$ at different synthesis pH give an isotherm typical for this group. This isotherm was not well defined, it had a hysteresis loop starting at the lower limiting relative pressure of $p/p_0 = 0.42$, and it did not close until the saturation pressure was reached. This effect most probably originates from the nonrigidity of the vesicle-like structure observed under TEM. However, there was a clear inflection point in the isotherm and at least a bimodal porosity with pore sizes in the range of 3–4.5 and 5–11 nm, respectively, was observed.

Discussion

Phase Behavior of the Decanoic Acid/CTAB Templated Silica. For dilute solutions where interaggregate interactions are of minor importance, a model has been developed to correlate the molecular geometry of the individual surfactant monomer to the observed aggregate structures.^{15,16} The packing parameter, P , is defined as $P = v/a_0l_c$, where v is the volume of the hydrophobic tail, l_c is the effective length of the surfactant, normally 80–90% of the fully extended hydrocarbon chain, and a_0 is the effective area of the hydrophilic headgroup. For P values of 0.33, 0.5, and 1.0, spherical, rodlike, and lamellar geometries are expected to form,

respectively. For ionic surfactants, a_0 is strongly dependent on the degree of dissociation of the headgroups and the ionic strength of the solution. A sphere-to-rod transition in micellar solutions has been observed previously for mixtures of cationic and anionic surfactants with asymmetrical hydrocarbon chain lengths,¹⁷ in agreement with the expected accompanying decrease in the value of the packing parameter.

When using a mixture of CTAB and decanoic acid, the strong electrostatic attraction between the positively charged CTA⁺ and the negatively charged decanoate will favor a close packing of the surfactants and therefore lead to a decrease in the area of the hydrophilic headgroup. This leads to an increase in the average packing parameter favoring threadlike over globular micellar geometries. The continuous increase in the d_{100} spacing with increasing decanoic acid/CTAB molar ratio also originates from this effect. Eventually, the increase in the packing parameter results in the hexagonal-to-lamellar phase transition observed at higher decanoic acid/CTAB molar ratios. The stabilization of surfactant assemblies with lower curvature is also seen in the increase in toluene solubilization capacity of the catanionic surfactant templated mesophase. This has previously been observed for solubilization of dodecane in catanionic micellar solutions.¹⁸ Furthermore, Kunieda et al.¹⁹ has described two possibilities for oil solubilization into micelles for nonionic surfactant systems. If the oil is preferentially solubilized in the palisade layer of the micelle, the effective area of the hydrophilic headgroup will increase without increasing the volume of the aggregate. If the oil, on the other hand, is solubilized into the core of the surfactant aggregates, the volume of the aggregates will increase without affecting the headgroup area. Toluene will be solubilized both in the core of the surfactant aggregate and in the palisade layer,^{20,21} and therefore both effects must be considered in our case. Furthermore, we have strongly adsorbing anionic polysilicate species present in our system, which can induce changes in the composition of the catanionic surfactant aggregates²² and therefore destabilize the decanoate/CTAB complex. Therefore, direct quantification of the combined influence of toluene and varying cationic/anionic surfactant ratios on the effective surfactant packing parameter of surfactant–silicate mesophases is difficult, and the comparisons should be considered qualitative in nature. In any case, the effects observed are similar in both cases, why such comparisons are justified.

Although the concept presented for easy adjustment of the packing parameter is a general one, it should be noted that decanoic acid has a pK_a value of about 4.7 and will consequently behave as a nonionic cosurfactant if the synthesis is carried out under acidic conditions. However, other anionic surfactants, like sodium dodecylsulfate (SDS), could be used as well. The value of being able to tune the preferential interfacial curvature

(15) Israelachvili, J. N.; Mitchell, D. J.; Ninham, B. W. *J. Chem. Soc., Faraday Trans. 2* **1976**, *72*, 1525.

(16) Israelachvili, J. N.; Mitchell, D. J.; Ninham, B. W. *Biochim. Biophys. Acta* **1977**, *470*, 185.

(17) Regev, O.; Khan, A. *J. Colloid Interface Sci.* **1996**, *182*, 95.

(18) Li, X.; Kunieda, H. *Langmuir* **2000**, *16*, 10092.

(19) Kunieda, H.; Ozawa, K.; Huang, K.-L. *J. Phys. Chem. B* **1998**, *102*, 831.

(20) Chaiko M. A.; Nagarajan R.; Ruckenstein E. *J. Colloid Interface Sci.* **1984**, *99*, 168.

(21) Dam, Th.; Engberts, J. B. N. F.; Kärthäuser, J.; Karaborni, S.; van Os, N. M. *Colloids Surf. A* **1996**, *118*, 41.

(22) Kabanov, V. A.; Yaroslavov, A. A.; Sukhishvili S. A. *J. Controlled Release* **1996**, *39*, 173.

of the surfactant assembly is not limited to silica, but can easily be extended to the synthesis of non-siliceous materials as well. This has been demonstrated for cationic–nonionic surfactant templated titania,²³ where the swelling of the hydrophobic portion of the inorganic–mixed surfactant 2D-hexagonal mesophase upon solubilization of trimethylbenzene could be fine-tuned by adjusting the ratio between the cationic and the non-ionic surfactant.

Effect of Aging. The fact that the lamellar phase disappears during the aging process could be due to a lamellar-to-hexagonal phase transition induced by the condensation of the inorganic framework, which has been observed previously for both silica/CTAB²⁴ and zirconia/CTAB²⁵ mesophases. However, in both these studies the syntheses were carried out in the absence of swelling agent. In the present case, the transformation of the lamellar phase to a swollen hexagonal phase, owing exactly the same d spacing as the swollen hexagonal phase observed for the as-synthesized material, seems highly unlikely. Therefore, two possibilities for the disappearance of the d_{001} reflection upon aging remain: (i) the lamellar phase transforms into a completely disordered phase as a result of silicate condensation or (less plausible) (ii) the lamellar phase is fragmented into a structure with a correlation length shorter than what is needed for a reflection to appear in the XRD. Even though the latter effect could be thought to be responsible for the appearance of the vesicular structures in the TEM image shown in Figure 7b, we believe that this is not the case, as discussed in the following.

Vesicular Structures. Surfactant–inorganic structures with a vesicular architecture have been observed previously for aluminophosphates and silica^{13,26–28} and calcium phosphate.²⁹ In the latter case, the vesicular structure was induced by electron irradiation and was probably not formed during the synthesis. However, the formation of vesicles in mixtures of cationic and anionic surfactants is well-documented. Raghavan et al.³⁰ have studied the phase behavior of a mixed catanionic surfactant system, with the C₁₈-tailed anionic surfactant sodium oleate and the cationic surfactant C_{*n*}TAB of different chain lengths. It was shown that, for C_{*n*}TAB with chain lengths $n = 10$ or 12 , wormlike micelles and bilayer structures (vesicles or lamellae) form. This is very close to our system, with C₁₆TAB and C₁₀-tailed decanoate instead of the C₁₈-tailed sodium oleate and C₁₂TAB, which could give support for a possible formation of vesicles in our system. However, we observed no vesicles in the completely transparent and homogeneous starting solution before addition of TEOS. It has been

shown that vesicles can be stabilized in mixtures of cationic and anionic surfactants at a 64/36 ratio if a strongly adsorbing counterion is used, due to an enhanced charge screening.³¹ The bromide counterions are replaced by anionic polysilicate species during the formation of the mesophase^{32,33} and therefore the formation of vesicular structures can be explained in our case.

The fact that fractions of a vesicle-like structure were also observed in a limited extent in the TEM images for the material synthesized at $o = 9.9$ and $m = 0$ indicates that the formation of the vesicular structure is not solely driven by the formation of the silicate–mixed catanionic surfactant mesophase. However, templating by emulsion droplets have been observed for surfactant–silicate mesophases synthesized under acidic conditions,³⁴ but has never been reported to occur under alkaline conditions. Despite the differences in hydrolysis and condensation kinetics under acidic and alkaline conditions, respectively, we cannot fully exclude the possibility of such an effect in our case as well, although we consider it to be fairly unlikely. However, this effect is under intense study and will be the focus of a forthcoming paper.³⁵

Summary

In conclusion, we have studied the properties of porous silica synthesized in the presence of a mixture of cationic and anionic surfactants as structure-directing agents and toluene as the swelling agent. The lower interfacial charge density of the mixed surfactant aggregates stabilizes structures of lower interfacial curvature and therefore facilitates a more controlled solubilization of toluene. It was shown that the pore size of the hexagonal phase could be controlled by changing the decanoic acid/CTAB and the toluene/CTAB molar ratios. Increasing the amounts of decanoic acid and toluene resulted in a hexagonal-to-lamellar phase transition over an intermediate region where the two phases coexist, which was observed by SAXS measurements. Extended, thin, and highly curved vesicular silica structures were observed in the TEM pictures, the occurrence of which is attributed to the use of catanionic surfactant mixtures as structure-directing agents in the synthesis.

Acknowledgment. The Finnish Technology Development Center, Tekes, is gratefully acknowledged for financial support. Andrew Root, Fortum Ltd., Finland, is gratefully acknowledged for carrying out the ²⁹Si NMR measurements. The authors thank Wolfgang Schmidt, Max-Planck Institut für Kohlenforschung, Mülheim/Ruhr, Germany, and Philip Llwellyn, CNRS, Marseille, France, for valuable comments on the manuscript.

CM0212430

(23) Czuryzkiewicz, T.; Kleitz, F.; Schüth, F.; Lindén, M., submitted.

(24) Monnier, A.; Schüth, F.; Huo, Q.; Kumar, D.; Margolese, D.; Maxwell, R. S.; Stucky, G. D.; Krishnamurthy, M.; Petroff, P.; Firouzi, A.; Janicke, M.; Chmelka, B. F. *Science* **1993**, *261*, 1299.

(25) Lindén, M.; Blanchard, J.; Schacht, S.; Schunk, S. A.; Schüth, F. *Chem. Mater.* **1999**, *11*, 3002.

(26) Tanev, P. T.; Pinnavaia, T. J. *Science* **1996**, *271*, 1267.

(27) Oliver, S.; Kuperman, A.; Coombs, N.; Lough, A.; Ozin, G. A. *Nature* **1995**, *378*, 47.

(28) Tanev, P. T.; liang, Y.; Pinnavaia, T. J. *J. Am. Chem. Soc.* **1997**, *119*, 8616.

(29) Yuan, Z. Y.; Liu, J. Q.; Peng, L. M.; Su, B. L. *Langmuir* **2002**, *18*, 2450.

(30) Raghavan, S. R.; Fritz, G.; Kaler, E. W. *Langmuir* **2002**, *18*, 3797.

(31) Yaacob, I. Y.; Bose, A. *J. Colloid Interface Sci.* **1996**, *178*, 638.

(32) Zana, R.; Frasc, J.; Soulard, M.; Lebeau, B.; Patarin, J. *Langmuir* **1999**, *15*, 2603.

(33) Frasc, J.; Lebeau, B.; Soulard, M.; Patarin, J. *Langmuir* **2000**, *16*, 9049.

(34) Schacht, S.; Huo, Q.; Voigt-Martin, I. G.; Stucky, G. D.; Schüth, F. *Science* **1996**, *273*, 768.

(35) Pevzner, S.; Regev, O.; Lind, A.; Lindén, M. *J. Am. Chem. Soc.* **2003**, *125*, 652.